



KINEMATIC ANALYSIS OF CONSTANT BREADTH CAM DRIVEN LINKAGES

¹Mert Eren AYGAHOĞLU , ²Ziya ŞAKA 

*Konya Technical University, Engineering and Natural Sciences Faculty, Mechanical Engineering Department,
Konya, TÜRKİYE*

¹meaygahoglu@ktun.edu.tr, ²zsaka@ktun.edu.tr

Highlights

- Different forms of constant breadth curves are obtained and given.
- Support functions of the curves are given.
- The kinematics of the constant breadth cam mechanisms are shown.
- Different positions of cam driven mechanisms are illustrated.
- The kinematics of constant breadth cam driven mechanisms are given.
- The effect of the fixed joint location of the mechanisms on kinematics are explained.



KINEMATIC ANALYSIS OF CONSTANT BREADTH CAM DRIVEN LINKAGES

¹Mert Eren AYGAHOĞLU , ²Ziya ŞAKA 

*Konya Technical University, Engineering and Natural Sciences Faculty, Mechanical Engineering Department,
Konya, TÜRKİYE*

¹meaygahoglu@ktun.edu.tr, ²zsaka@ktun.edu.tr

(Geliş/Received: 10.02.2023; Kabul/Accepted in Revised Form: 01.04.2023)

ABSTRACT: Several constant breadth curves are defined that can be used as cam profiles in constant breadth cam mechanisms that are closed cam mechanisms. There are two objectives for this study. One of them is to study the kinematic analysis of different type of constant breadth cam mechanisms. The other objective is to obtain a dwell period for constant breadth cam driven linkages that is impossible for a standard cam mechanism. A general kinematic analysis of a constant breadth cam mechanism with translating flat-faced follower was carried out with the principle of kinematic inversion. With the results, the kinematic analyses of the constant breadth cam driven inverted slider crank mechanism and four bar mechanism were examined in detail and a general method is given for all constant breadth cam profiles and cam driven linkages. It has been seen that a dwell period of 45° (with the fixed joint coordinates as $x_n = 18$ mm and $y_n = 8.5$ mm) and 40° (with the fixed joint coordinates as $x_n = 18.5$ mm and $y_n = 8.5$ mm) can be obtained in designed cam driven four bar and inverted slider crank mechanism respectively. After the displacement analysis, some velocity and acceleration analysis examples are given by taking the derivative of displacement. Similar kinematic analyses are possible for cam-driven mechanisms with more links. Also, it has been seen that changing the location of fixed joint of the cam profile can affect the displacement, velocity and acceleration graphics of the mechanism. With this, the dwell period can be changed too.

Keywords: Support Function, Constant Breadth Curve, Constant Breadth Cam Mechanism, Cam Driven Mechanism, Kinematic Analysis

1. INTRODUCTION

Profiles with a curved surface that either have a point or line contact are called cam and the mechanisms that convert the circular motion into alternative motion and have cams as a link are called cam mechanisms.

Cam mechanisms play an important role in modern automatic machines due to their high speed and high precision. The transmission accuracy, stability and lifetime of a cam-follower system are highly related to its kinematic and dynamic performances, while the kinematic and dynamic performances depend essentially on the mathematical characteristic of the cam profile[1].

One of the most important problems to be considered in cam mechanisms is to ensure continuous contact between the follower and the cam profile. In this respect, these mechanisms are divided into form closed cam mechanisms and force closed cam mechanisms. Force closed cam mechanisms, in which pre tension elements such as springs are used, are the most widely used cam mechanisms in practice. An important advantage of constant breadth cam mechanisms, which are form closed cam mechanisms, compared to force closed cam mechanisms is that they provide simplicity and cheapness in construction since there is no need to use pre tension elements such as springs. Therefore, this type of cam mechanisms are highly preferred systems in many applications that do not require high precision at medium speed [1], [2].

There are many studies in the literature on constant breadth curves that can be used as cam profiles in constant breadth cam mechanisms. An extensive list of literature on this topic is given in reference [3]. Theoretical information on constant breadth curves and constant breadth bodies are also included in the same resource.

*Corresponding Author: Mert Eren AYGAHOĞLU, meaygahoglu@ktun.edu.tr

Rabinowitz [4] and many other researchers [2], [3], [5], [6] used support functions to obtain constant breadth curves, after that, they studied the parametric and polynomial equations of the curves. They also showed that many different constant breadth curves could be obtained by giving different values to the equation variables used. H. L. Resnikoff, in his study [7], studied the constant breadth curve equation and the parameters (support function, the radius of curvature, curve arc length, curve area, etc.) of constant breadth curves by using the Fourier series. The author also stated that he obtained many constant breadth surfaces based on the Fourier series. In a similar study, Andrew David Irving [8] calculated the parameters of constant breadth curves without using the Fourier series and simplified the radius of curvature formula to be limited to constant breadth curves. The author also stated that he obtained some theoretical results about constant breadth curves. In his comprehensive book, Harold A. Rothbart [2] examined the dynamic analysis, synthesis, manufacturing methods of cam mechanisms with different types and properties and differences of cam mechanisms to other mechanisms. The author dealt with many geometric, kinematic, and dynamic concepts related to cam mechanisms in detail and gave theoretical and practical information about them. Chatchawan Panraksa and Lawrence C. Washington [9] stated that there are isolated points outside the original curve in the constant breadth curve that Rabinowitz studied, and they tried to construct that constant breadth curve without isolated points. Lucie Paciotti [10] studied the Reuleaux triangle, a circle and Rabinowitz's constant diameter curve with equal breadth. The author stated that these curves could be obtained and the difference between these curves can be determined by creating shadow functions with the principle of shedding light from a certain direction. As a result of the author's work, Lucie Paciotti stated that the parameters of any differentiable curve could be found with the shadow function of that curve. In their study, S. G. Dhande and N. Rajaram [11] studied the kinematic analysis of constant breadth cam mechanisms using two different constant breadth cam profiles and two different follower types, translating and oscillating follower. The first of the cam profiles is the profile consisting of Reuleaux type circular arcs. The other is the three cusped hypocycloid-based constant breadth cam profile previously introduced by Euler [3]. In the analysis of the second profile, they used geometric properties of the hypocycloid. Zhang Jinjiang [12] stated that he found a new type of constant breadth curve using polar tangent coordinates in his work. The author analyzed the parameters of this type of curve mathematically. Zhang Jinjiang stated that in convex constant breadth curves, symmetrical constant breadth curves are mostly obtained with circular arcs, and asymmetric constant breadth curves are obtained mostly with Reuleaux triangles. Giorgio Figliolini and Pierluigi Rea [13], examined motion analysis in mechanisms that use the Reuleaux triangle and the modified Reuleaux triangle. They stated that they did the motion analysis of mechanisms by formulating suitable algorithms as a result of many simulations. From there they analyzed a square-hole drill that makes use of the modified Reuleaux triangle with a rounded corner, along with the motion analysis of the Wankel engine. Ş. Yüzbaşı and M.Karaçayır [14] studied to obtain a solution for first order linear differential equation system characterizing curves of constant breadth in Euclidean 3-space. They stated that they outlined a numerical method for the solution. The method they used relies on transforming the given problem to a system of linear equations, whose solution yields three polynomials of degree N as the approximate solutions. According to the obtained numerical results, increasing the parameter N improves the accuracy of the solution. The authors also stated that the proposed method can be used to solve models of similar type with a high accuracy. Honda Satoshi and Tanaka Shun [15] stated that they integrated the reduction mechanism into the constant breadth cam mechanism to be used in the inchworm engine. They analyzed the relational expression between rotations of the constant breadth cam and the engaging approach of the inchworm motion. Also they examined the performances of the reduction mechanism integrated into the constant breadth cam mechanisms. Liangwen Wang and his friends studied [16] the configuration of a bionic horse robot for equine-assisted therapy. The mechanism's structure is that a single-leg system with two degrees of freedom (DOFs) is driven by a cam linkage, and it can adjust the span and height of the leg end-point trajectory. In their analysis, they stated that using a constant breadth cam driven four bar mechanism simplifies the robot's control system. Asgari et al. [17] designed and manufactured a wearable passive cam-driven shoulder exoskeleton. They used modular spring -cam-wheel module that generates an

assistive force to compensate the shoulder elevation moment due to gravity. They also performed a pilot biomechanics study to evaluate the effect of the exoskeleton on muscle activity and shoulder kinematics. After obtaining the results, they stated that, the exoskeleton they proposed can assist shoulder movement against gravity. Enrique and Irene [18], designed, manufactured and measured metallic and plastic constant breadth cam mechanisms. They compared the cams in terms of dimensional accuracy and surface finish. Their aim was to evaluate if it would be possible to replace metallic cam with a plastic one for a short period of time. According to the results they obtained, they stated that, the replacement is only recommended for applications of low-power transmission. Artobolevsky [19], gave many examples of cam mechanisms in practice, including constant breadth cam mechanisms, and explained their working principles. Mechanisms similar to the constant breadth cam driven linkages, which will be discussed in this study, are also included in Artobolevsky's book.

The aim of this paper is to study the kinematic analysis of different type of constant breadth cam mechanisms and obtain a dwell period for constant breadth cam driven linkages that is impossible for a standard cam mechanism. In this study, firstly, the theory about constant breadth curves is discussed and several constant breadth curves that can be used as cam profiles in constant breadth cam mechanisms are obtained. Then a general kinematic analysis of a constant breadth cam mechanism with translating flat-faced follower was studied with the principle of kinematic inversion. With the results, the kinematic analysis of the constant breadth cam driven four bar and inverted slider crank mechanism were examined in detail. In kinematic analysis, examples related to velocity and acceleration analysis are given after displacement analysis. Similar kinematic analysis can be performed for cam-driven mechanisms with more links.

2. CONSTANT BREADTH CURVES AND SUPPORT FUNCTION

The equation of the family of lines tangent to a continuous, closed and convex planar curve can be written as:

$$x \cos \theta + y \sin \theta = p(\theta) \quad (1)$$

Here x and y are the coordinates of the tangent point and θ is the angle between the perpendicular side joining the curve center to the tangent and the horizontal side. The function $p(\theta)$ defined in this way is called the support function and gives the length of the said perpendicular [4]–[6].

The curve in question can be defined as the envelope of this line family [20]. If the envelope theory is applied, the parametric equation of the curve will be as follows:

$$x(\theta) = p(\theta) \cos \theta - p'(\theta) \sin \theta \quad (2)$$

$$y(\theta) = p(\theta) \sin \theta + p'(\theta) \cos \theta \quad (3)$$

For a curve to be a constant breadth curve, the perpendicular distance between its tangent at any point and its parallel tangent on the other side of the curve must be the same. (Figure 5). This condition is expressed as:

$$w = p(\theta) + p(\theta + \pi) = \text{constant} \quad (4)$$

Where the w represents the width of a constant breadth curve. The radius of curvature (ρ) must satisfy the following condition to prevent undercutting on a constant breadth curve:

$$\rho = \frac{(x'^2 + y'^2)^{1.5}}{x'y'' - y'x''} > 0 \quad (5)$$

If equations 2 and 3 are substituted in equation 5 and simplified [3], [21]:

$$\rho = p(\theta) + p''(\theta) > 0 \quad (6)$$

In order for this equation to be satisfied, the support function should be as follows [5] or similar trigonometric form:

$$p(\theta) = a \cos^2\left(\frac{k\theta}{2}\right) + b \sin^2\left(\frac{l\theta}{2}\right) + c \quad (7)$$

The a , b , c and k are constants. If $a = b = 0$ and $c \neq 0$ are taken here, the curve becomes a circle. If $b=0$, $k=3$ and $a \neq 0$, $c > 0$, the simplest three-lobed constant breadth curve [4] is obtained. The parameters, $a = 4$, $k = 3$, and $c = 23$ are chosen to be suitable constant breadth curve and be the same width as the other curves. Obtained constant breadth curve from these parameters is given in Figure 1.

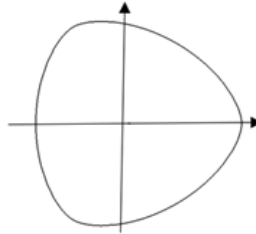


Figure 1. Constant breadth curve

Different forms of constant breadth curves can be obtained by using trigonometric functions. Support functions of four different constant breadth curves are given as an example below. All of these satisfy equations 4 and 5. The curves obtained with trial-and-error method, some symmetrical and others asymmetrical, are shown in Figure 2.

- a. $p(\theta) = \sin 3\theta + \frac{13}{15} \sin 3\theta \cos 2\theta + 25$
- b. $p(\theta) = 2\cos^2 2\theta \sin^3 \theta + 25$
- c. $p(\theta) = 2\sin(\pi \cos \theta) \cdot \cos(\pi \sin \theta) + 25$
- d. $p(\theta) = \sin 2\theta \cos 3\theta + \cos 3\theta + 25$

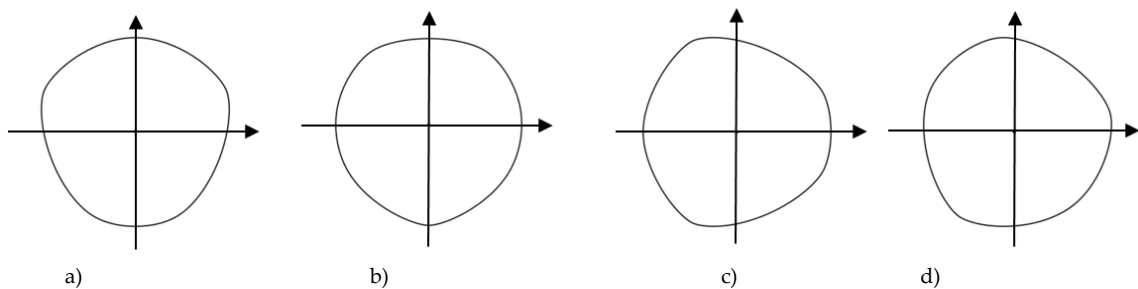


Figure 2. Examples of constant breadth curves used as a constant breadth cam profile

Constant breadth curves can also be expressed by a closed-form polynomial equation [4], [8]. The above parametric expressions are preferred for ease of processing mathematically.

3. CONSTANT BREADTH CAM MECHANISMS

Constant breadth cam mechanisms are generally form closed mechanisms. A constant breadth cam profile can be created in two ways; the first is the Reuleaux triangle method. In this method, the profile is created with circular arcs. The second method uses a suitable constant breadth curve as the cam profile. All of the constant breadth curves mentioned above can be used as cam profiles. In the mechanism, the cam is the actuating member, the member that the cam moves can make a translating movement or an oscillating movement, as in Figure 3. In such a mechanism, it is sufficient that the cam and the 3rd link frame that the cam actuates are tangent at two points in the direction perpendicular to the movement direction; there is no need for contact since there is no movement in the other direction. Thus, a two degree of freedom cam pair is formed, and the total degree of freedom of the mechanism becomes $F=1$ according to the Kutzbach criterion [22].

A constant breadth cam driven linkage can also be formed in a different structure, as in Figure 4. According to the structure of such a four bar mechanism, there will be a mechanism similar to a four bar,

inverted slider crank, or slider crank mechanism. Here, the frame of the 3rd link must be in contact with the constant breadth cam profile from four points in two parallel directions perpendicular to each other, as in Figure 4, because the movement of the 3rd link in both directions is possible. Thus, the cam pair has one degree of freedom, and the total degree of freedom of the mechanism becomes $F=1$ [22]. Here, the perpendicular distances between the parallel tangents must be equal to the constant breadth (w) of the cam in both directions; that is, the frame will be in the form of a square.

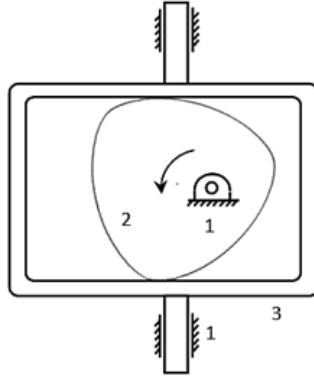


Figure 3. Constant breadth cam mechanism with translating flat-faced follower

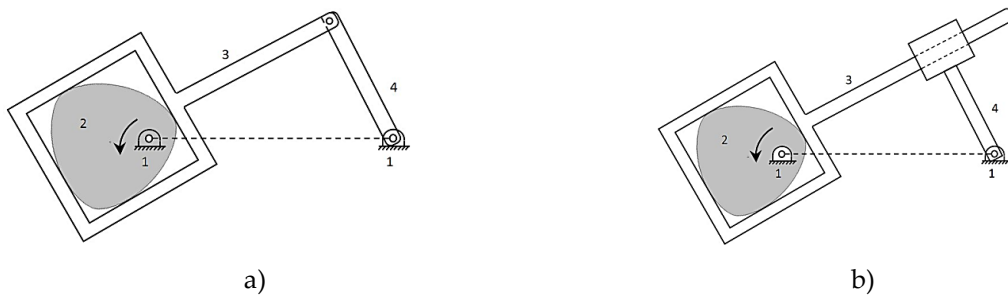


Figure 4. Cam driven mechanisms a) Four bar mechanism b) Inverted slider crank mechanism

In the cam mechanism in Figure 3, the 3rd link, which makes translational movement, is always tangent to the constant breadth cam profile. The kinematic inversion principle can be applied to obtain the displacement equation of this link. For this, considering that the cam is fixed and the 3rd link rotates around it, as seen in Figure 3, the perpendicular distance of the link line tangential to the cam at any position to the cam rotation center (A) will be the linear displacement s of the link.

The slope of the tangent line "m" at point P,

$$m = \frac{dy}{dx} = \frac{dy/d\theta}{dx/d\theta} = \frac{y'}{x'} \quad \text{and the line equation,}$$

$$y = y_t + m(x - x_t) \quad \text{is in the form.}$$

The slope of the perpendicular drawn from the fixed joint $A(x_n, y_n)$ of the cam to the tangent $m \cdot m' = -1$, $m' = -1/m$ and its equation, $y = y_n + m'(x - x_n)$ is in the form.

The intersection point D of these two lines is found from the joint solution of the equations below:

$$x_d = \frac{m^2 x_t + m(y_t - y_n) + y_n}{(1 + m^2)} \quad (8)$$

$$y_d = \frac{m^2 y_n + m(x_n - x_t) + y_t}{(1 + m^2)} \quad (9)$$

at any θ value, the coordinates x_t and y_t and their derivatives x'_t , y'_t are calculated via equations 2 and 3. The linear position "s" of 3rd link is equal to the length of AD:

$$s = s(\theta) = \sqrt{(x_d - x_n)^2 + (y_d - y_n)^2} \quad (10)$$

Here, the point coordinates are determined by the axis set at the cam center (Figure 5). Example displacement graphics of the cam profiles in Figure 2 with fixed joint coordinates $x_n=16$ mm and $y_n=7.5$ mm are given in Figure 6.

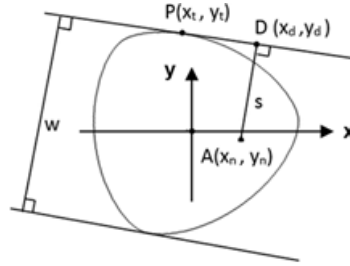


Figure 5. Constant breadth cam and its tangents

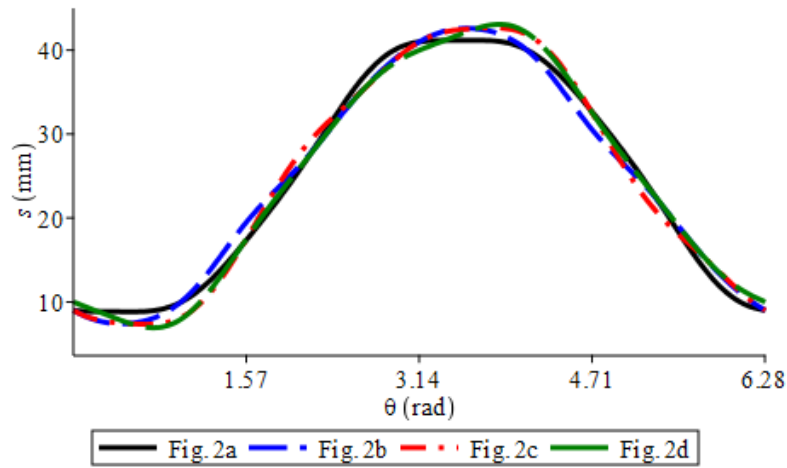


Figure 6. Follower displacement graphs of the constant breadth cam mechanism with translating flat-faced follower in Figure 3

3.1. Constant Breadth Cam Driven Four bar Mechanism

Figure 7 results if the four bar mechanism, the first of the cam driven four bar mechanisms in Figure 4, is drawn schematically at any position of the constant breadth cam. Here, points A, B, and D are the revolute pair centers of the cam, 3rd, and 4th link, respectively. The side length of the square frame of the 3rd link surrounding the cam is equal to the constant breadth of the cam, w . It is assumed that the center of the 34 revolute pair connecting the 3rd and 4th link is connected to this frame perpendicularly from the G, which is the midpoint of the square edge, because this is the most appropriate in terms of the balance of forces and dynamics. Even if the connection is made from a different point, analysis can be made by considering that there is a connection in this way geometrically. Let C be the point where the GD direction intersects the horizontal fixed link line of AB. The perpendicular length drawn from the point A, which is the rotation center of the constant breadth cam, to the other side of the frame is determined by the expression $s(\theta)$ in equation 10. With this direction, $s_1 = w - GF$, which is the perpendicular distance of point F to the other side of the frame, is equal to the perpendicular distance of point A to the same edge, as can be seen from Figure 7, this perpendicular distance is equal to the value $s(\theta + \pi/2)$.

in perpendicular triangle CAF, $CA = \frac{AF}{\sin\theta_3}$ and taking into account the frame geometry,
 $AF = s - 0.5w$, $CF = CA \cos\theta_3$ and $CD = w + r_3 - s_1 + CF$ is written.

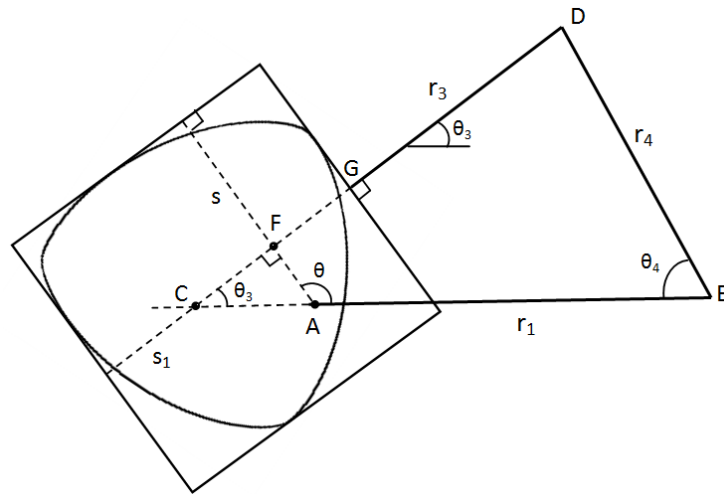


Figure 7. Schematic illustration of a constant breadth cam driven four bar mechanism

If the horizontal and vertical projections of the sides of the CDB triangle are written;

$$r_4 \cos \theta_4 + CD \cos \theta_3 = r_1 + CA \quad (11)$$

$$r_4 \sin \theta_4 = CD \sin \theta_3 \quad (12)$$

If these two expressions are arranged, leaving the r_4 terms on the left and squared and summed side by side, only θ_3 remains in the equations:

$$r_4^2 = CD^2 + (r_1 + CA)^2 - 2CD(r_1 + CA) \cos \theta_3 \quad (13)$$

After equation 13 is arranged, substituting $\tan \frac{\theta_3}{2}$ with t yields a quadratic equation for θ_3 :

$$at^2 + 2bt + c = 0 \quad (14)$$

Here,

$$a = (r_1 + w + r_3 - s_1)^2 + (s - 0.5w)^2 - r_4^2 \quad (15)$$

$$b = 2r_1(s - 0.5w) \quad (16)$$

$$c = (r_1 - w - r_3 + s_1)^2 + (s - 0.5w)^2 - r_4^2 \quad (17)$$

$$\theta_3 = 2 \arctan \left[\frac{-b + \sqrt{b^2 - ac}}{a} \right] \quad (18)$$

For the mechanism configuration to be as in Figure 7, the (+) sign should be used in this expression. The (-) sign indicates reverse configuration. At any value of the cam angle θ , the values $s(\theta)$ and $s_1 = s(\theta + \pi/2)$ be calculated, and the corresponding θ_3 value can be found. If the discriminant is negative, there is no real solution for θ_3 at the θ value, meaning that the mechanism cannot make a full rotation.

In the two positions where the CD direction passes through the fixed joint point A, the mechanism passes through dead-centre positions, where points A and F overlap. In the dead-centre position where point C is to the right of point A, the values of θ and θ_3 are equal; it can be seen from Figure 7 that $\theta = \theta_3 + \pi$ when to the left.

To find the value of θ_4 , arranging equation 12 and substituting $\tan \frac{\theta_4}{2}$ with p ;

$$ep^2 - 2r_4p + e = 0, \quad \text{here,}$$

$$e = [w + r_3 - s_1 + (s - 0.5w)\cot\theta_3]\sin\theta_3 \tag{19}$$

$$\theta_4 = 2\arctan \left[\frac{r_4 - \sqrt{r_4^2 - e^2}}{e} \right] \tag{20}$$

The angular displacements of the links in the mechanism will vary according to the cam and link lengths and the selected cam profile. When the coordinates of the fixed joint are taken as $x_n=18$ mm and $y_n=10$ mm, for the constant breadth cam profile in Figure 1, the mechanism positions are shown in Figure 8 for the cam rotation angle $\theta = 0^\circ$, $\theta = 100^\circ$ and $\theta = 280^\circ$. The link lengths and the constant breadth of the cam are taken as $r_1 = 70$ mm, $r_3 = 65$ mm, $r_4 = 90$ mm and $w = 50$ mm.

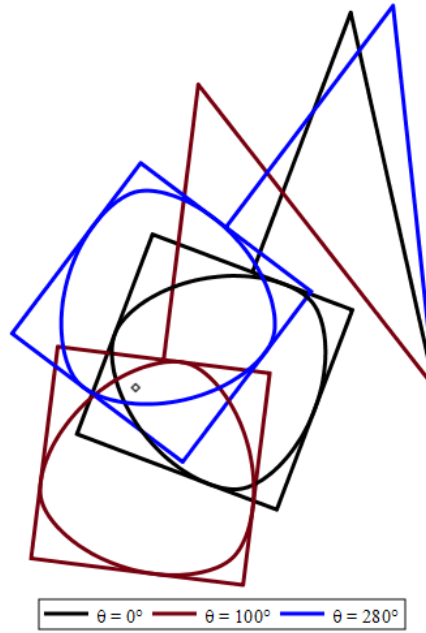


Figure 8. Positions of a constant breadth cam driven four bar mechanism

Taking link lengths $r_1 = 80$ mm, $r_3 = 70$ mm, $r_4 = 105$ mm and fixed joint coordinates $x_n = 18$ mm, $y_n = 8.5$ mm, in the mechanism, graphs showing the change of θ_4 angle with respect to cam angle θ are given in Figures 9a and 9b, respectively, for the cam profile in Figure 1 and some cam profiles in Figure 2 ($w=50$ mm).

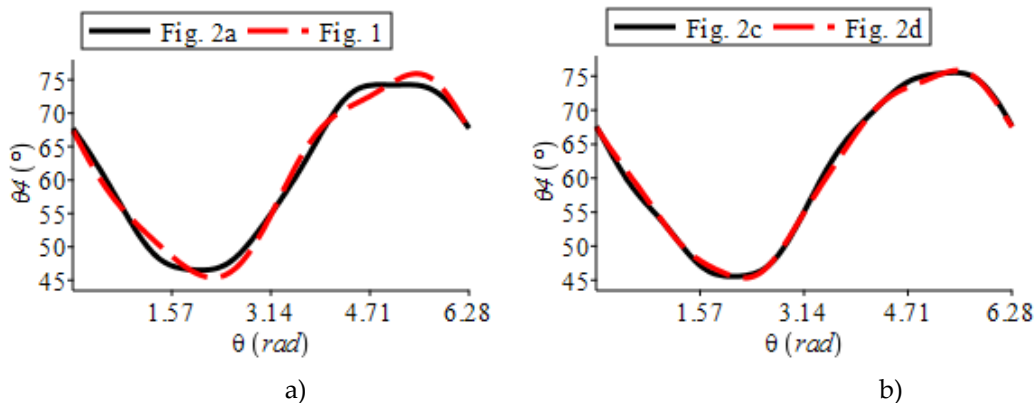


Figure 9. Constant breadth cam driven four bar mechanism a) θ_4 displacement graphs of cam profiles in Figure 1 and 2a b) θ_4 displacement graphs of cam profiles in Figure 2c and 2d

In this type of constant breadth cam driven four bar mechanism, a dwell period can be obtained in the 4th link. If the coordinates of the fixed joint taken as $x_n = 18$ mm and $y_n = 8.5$ mm for the cam profile in Figure 2a in the mechanism given as an example above, a dwell period of approximately 45° occurs around

$\theta = 3\pi/2$ rad in the movement of the 4th link, as seen in the black graph of Figure 9a. It is impossible to achieve such a dwell period in the classical four bar mechanism. This feature also has potential value for the practical use of this constant breadth cam driven mechanism.

The angular velocities of the 3rd and 4th links can be found by taking the derivatives of equations 11 and 12 to cam rotation angle. If the derivative is taken in Equation 12;

$$r_4\omega_4\cos\theta_4 = [-\omega_2s'_1 + \omega_2s' \cot\theta_3 - (s - 0.5w)\omega_3(1 + \cot^2\theta_3)]\sin\theta_3 + [w + r_3 - s_1 + (s - 0.5w) \cot\theta_3] \omega_3\cos\theta_3 \tag{21}$$

here $s' = ds/d\theta$, $s'_1 = ds_1/d\theta$, $\omega_2 = d\theta/dt$, ω_2 is the angular velocity of the cam, which is 2nd link.

In Equation 11, there is also an equation for the angular velocity ω_4 by similarly taking the derivative, and angular velocity expression is obtained from these two equations. Since the expression is long, it is given in Appendix 1.

In these equations, angular acceleration expressions are obtained by taking one more derivative to cam rotation angle. Taken $\omega_2 = 1$ unit, the graphics of said mechanism's angular velocity (ω_4) and angular acceleration (α_4) are given in Figure 10 and 11, respectively.

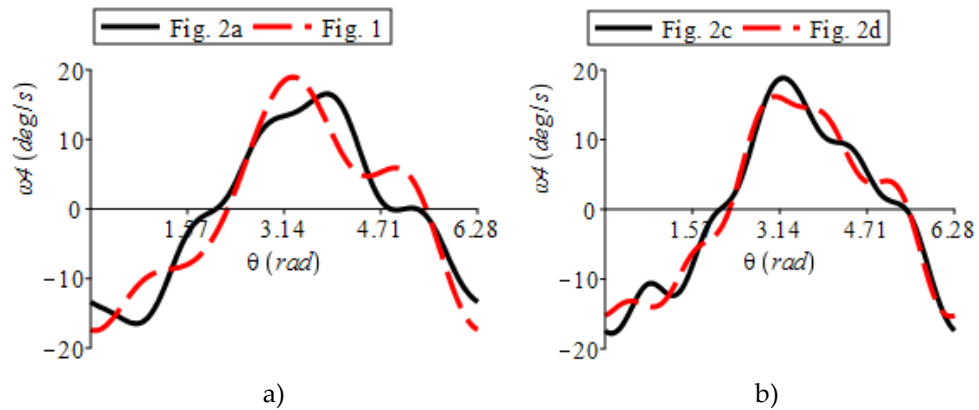


Figure 10. Constant breadth cam driven four bar mechanism a) ω_4 angular velocity graphs of cam profiles in Figure 1 and 2a b) ω_4 angular velocity graphs of cam profiles in Figure 2c and 2d

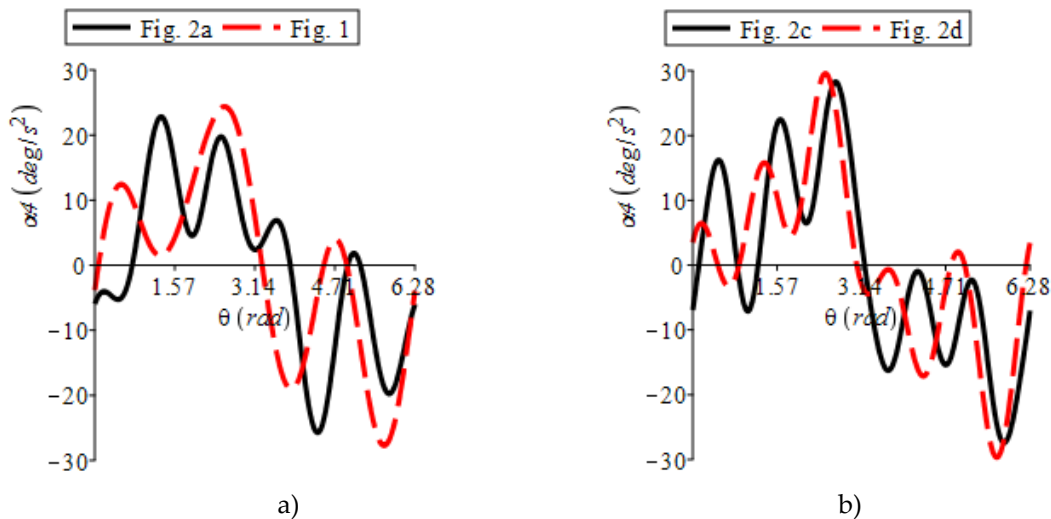


Figure 11. Constant breadth cam driven four bar mechanism a) α_4 angular acceleration graphs of cam profiles in Figure 1 and 2a b) α_4 angular acceleration graphs of cam profiles in Figure 2c and 2d

3.2. Constant Breadth Cam Driven Inverted Slider Crank Mechanism

The structure of the constant breadth cam driven inverted slider crank mechanism is shown in Figure 4b. Here, pair 34 is a prismatic pair, 3rd link makes a sliding motion on the 4th link. Unlike the four bar mechanism above, here the length of 3rd link (r_3) is variable. The schematics of the mechanism are completely similar to that of Figure 7. As in the classical inverted slider crank mechanism, the directions of 3rd and 4th links are always perpendicular to each other, and if this perpendicularity is taken into account in Figure 7, it can be seen that $\theta_3 + \theta_4 = 90^\circ$. In this mechanism, equations 11 and 12 for displacement analysis are written similarly.

If $90 - \theta_4$ is written and edited instead of θ_3 in equation 12;

$$r_4 \sin \theta_4 = [w + r_3 - s_1 + (s - 0.5w)\tan\theta_4]\cos\theta_4 \quad (22)$$

$$r_3 = \frac{r_4 \sin \theta_4 - w \cos \theta_4 + s_1 \cos \theta_4 - s \sin \theta_4 + 0.5w \sin \theta_4}{\cos \theta_4} \quad (23)$$

If the expression r_3 is substituted in equation 11 and simplified;

$$r_1 \cos \theta_4 - r_4 + s - 0.5w = 0 \quad (24)$$

If the $k = \tan \frac{\theta_4}{2}$ transformation used in the solution of trigonometric equations is arranged;

$$f k^2 - g = 0, \text{ here,} \quad (25)$$

$$f = r_1 - s + 0.5w + r_4, \quad g = r_1 + s - 0.5w - r_4 \quad (26)$$

From equation 25, θ_4 is simply calculated;

$$\theta_4 = 2\arctan\sqrt{g/f} \quad (27)$$

For the configuration of the mechanism to be as in Figure 7, the positive root in equation 25 should be used; the negative root denotes the reverse configuration.

When the coordinates of the fixed joint of the cam profile in Figure 1 are taken as $x_n=12$ mm, $y_n=12$ mm, for the cam rotation angle $\theta = 55^\circ, 120^\circ$ and 230° the mechanism positions are shown in Figure 12. The link lengths and the constant breadth of the cam are taken as $r_1 = 110$ mm, $r_4 = 70$ mm and $w = 50$ mm.

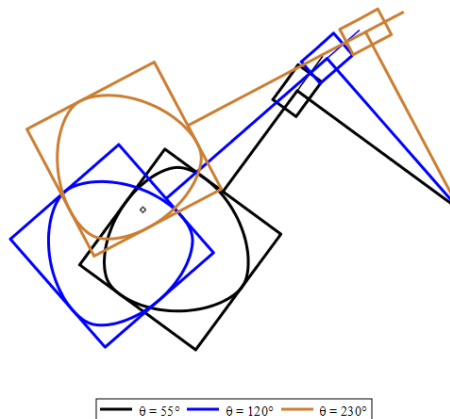


Figure 12. Positions of constant breadth cam driven inverted slider crank mechanism

Taking link lengths $r_1 = 130$ mm, $r_4 = 70$ mm and fixed joint coordinates $x_n = 18.5$ mm, $y_n = 8.5$ mm in the mechanism, graphs showing the change of θ_4 angle with respect to cam angle θ are given in Figures 13a and 13b, respectively, for the cam profile in Figure 1 and some cam profiles in Figure 2. ($w=50$ mm)

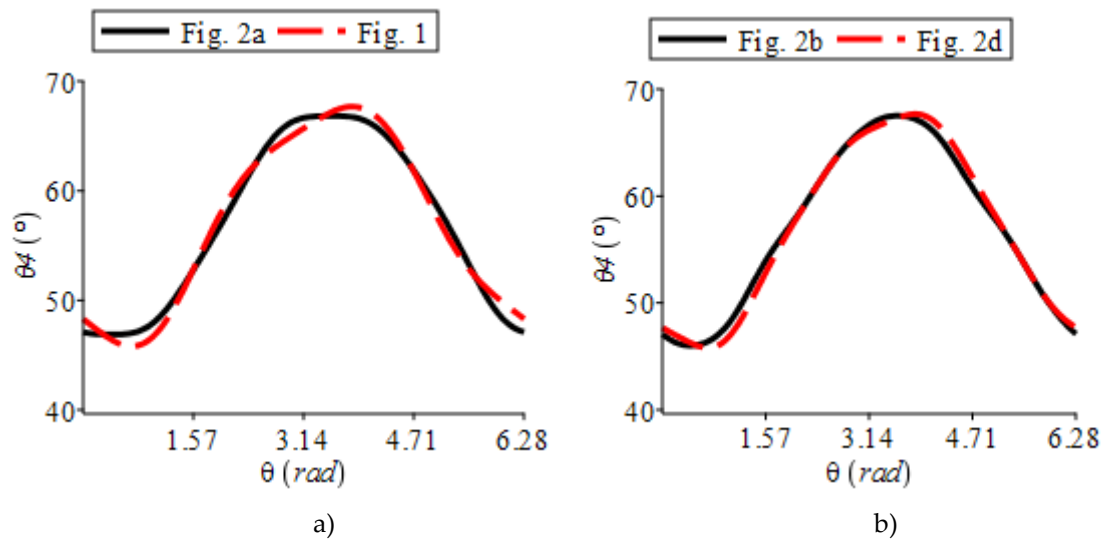


Figure 13. Constant breadth cam driven inverted slider crank mechanism a) θ_4 displacement graphs of cam profiles in Figure 1 and 2a b) θ_4 displacement graphs of cam profiles in Figure 2b and 2d

As with the constant breadth cam driven four bar mechanism, the constant breadth cam driven inverted slider crank mechanism can be obtained dwell period. If the coordinates of the fixed joint taken as $x_n = 18.5$ mm and $y_n = 8.5$ mm for the cam profile in Figure 2a in the mechanism given as an example above, a dwell period of approximately 40° occurs around $\theta = \pi$ rad in the movement of the 4th link, as seen in the black graph of Figure 13a.

In Equation 24, the angular velocity expression (ω_4) of 4th link can be found simply by taking the derivative to cam rotation angle:

$$r_1 \omega_4 (-\sin \theta_4) + s' \omega_2 = 0, \tag{28}$$

here, $s' = ds/d\theta$, $\omega_2 = d\theta/dt$, ω_2 is the angular velocity of the cam.

$$\omega_4 = s' \omega_2 / (r_1 \sin \theta_4) \tag{29}$$

Here, by taking $\omega_2 = 1$ unit, which is, normalizing according to ω_2 , the angular velocity graphs of ω_4 for the above mentioned mechanism are given as an example in Figure 14, respectively.

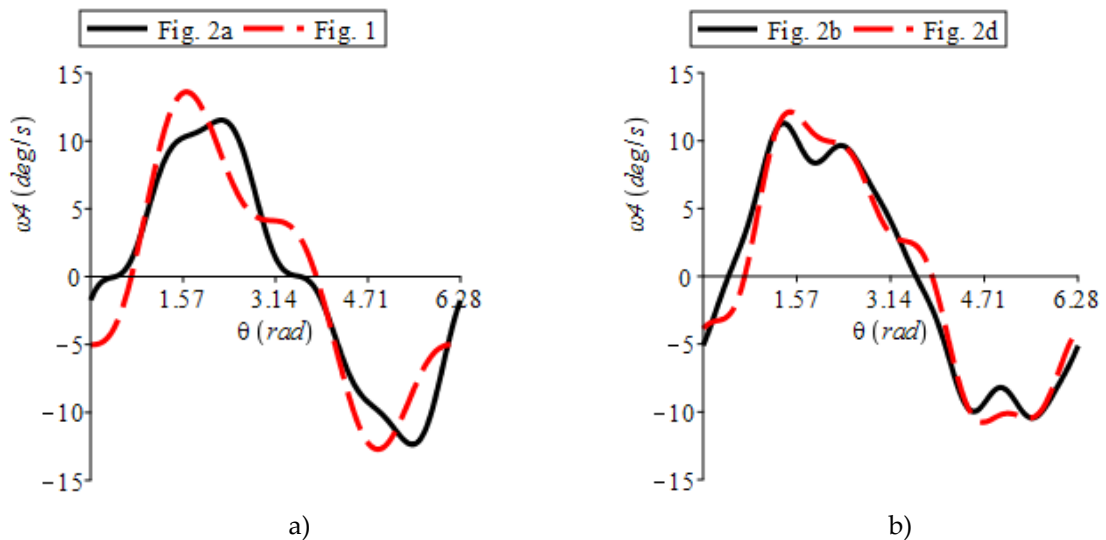


Figure 14. Constant breadth cam driven inverted slider crank mechanism a) ω_4 angular velocity graphs of cam profiles in Figure 1 and 2a b) ω_4 angular velocity of cam profiles in Figure 2b and 2d

If the angular velocity of the cam ω_2 is assumed to be constant and the derivative is taken once more with respect to cam rotation angle in equation 28, the angular acceleration expression of 4th link (α_4) is found:

$$r_1\alpha_4(-\sin\theta_4) + (r_1\omega_4^2\cos\theta_4) + s''\omega_2^2 = 0 \quad (30)$$

here, $s'' = d^2s/d\theta^2$

$$\alpha_4 = (s''\omega_2^2 - r_1\omega_4^2\cos\theta_4)/(r_1\sin\theta_4) \quad (31)$$

By taking $\omega_2 = 1$ unit α_4 angular acceleration graphs for the above mechanism are given as an example in Figure 15, respectively.

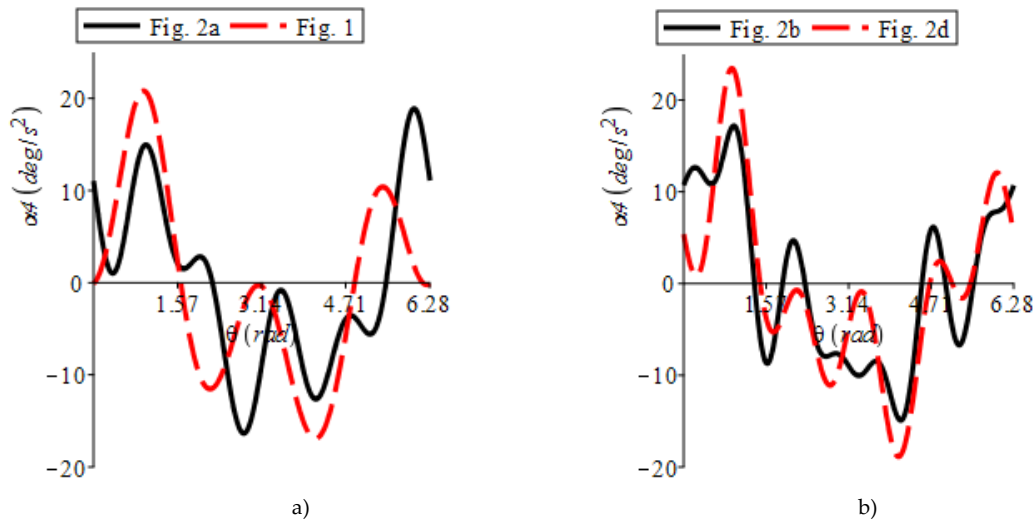


Figure 15. Constant breadth cam driven inverted slider crank mechanism a) α_4 angular acceleration graphs of cam profiles in Figure 1 and 2a b) α_4 angular acceleration of cam profiles in Figure 2b and 2d

Analysis of a constant breadth cam driven slider crank mechanism with a similar construction can be done in a similarly.

Nomenclature can be found in Appendix 2.

4. CONCLUSION AND DISCUSSION

There are many studies on constant breadth cam mechanisms. The vast majority of existing studies are also related to Reuleaux type mechanisms. A method based on hypocycloid geometry was used in the kinematic analysis of the hypocycloid-based constant breadth cam mechanism, which was considered together with the Reuleaux type cam mechanism. In this study, a general method valid for all constant breadth cam profiles and cam driven linkages is presented. This method can be applied similarly in such linkages that have more links.

As shown by the examples here, different motions with different characteristics can be obtained with different constant breadth cam profiles. Also, the motion profile can be changed by changing the location of the fixed joint of the cam profile. It is also possible to obtain dwell motion with appropriate lengths in the mechanism.

Declaration of Ethical Standards

The authors mentioned in the manuscript have agreed for authorship, read and approved the manuscript, and given consent for submission and subsequent publication of the manuscript.

Credit Authorship Contribution Statement

Mert Eren AYĞAHOĞLU: The author has done research, analysis and writing.

Ziya ŞAKA: The author has done conceptualization, review and editing.

Declaration of Competing Interests

The authors declared no potential conflicts of interest with respect to the research, authorship, and/or publication of this article.

Funding / Acknowledgements

The authors received no financial support for the research, authorship, and/or publication of this article.

APPENDICES

Appendix 1

The formulation of the angular velocity ω_4 of an exemplary constant breadth cam driven four bar mechanism is given below from the derivatives of equations 11 and 12 to cam rotation angle :

$$\omega_4 = \frac{[(w+r_3-s_1)s'_1+(0.5w-s)s']\sin(\theta_3-\theta_4)}{r_4[(w+r_3-s_1)(\sin^2\theta_4-\sin^2\theta_3)+0.5(s-0.5w)(\sin 2\theta_4-\sin 2\theta_3)]}\omega_2 \quad (34)$$

Appendix 2

Table 1. Nomenclature

θ_i	Rotation angle
s	Displacement of follower
s_1	The distance s rotated by 90°
$p(\theta)$	Support function
ρ	Radius of curvature
x_n	x coordinate of fixed joint
y_n	y coordinate of fixed joint
r_i	Link length
w	Constant breadth of the cam
m	The slope of the tangent line
m'	The slope of the perpendicular to the tangent

REFERENCES

- [1] J. Yu, H. Luo, J. Hu, T. V. Nguyen, and Y. Lu, "Reconstruction of high-speed cam curve based on high-order differential interpolation and shape adjustment," *Appl Math Comput*, vol. 356, pp. 272–281, Sep. 2019, doi: 10.1016/j.amc.2019.03.049.
- [2] H. A. Rothbart, "Cam Design Handbook: Dynamics and Accuracy," 2004, doi: 10.1036/0071433287.
- [3] H. Martini, L. Montejano, and D. Oliveros, *Bodies of Constant Width*. Cham: Birkhäuser, 2019.
- [4] S. Rabinowitz, "A Polynomial Curve of Constant Width," *MathPro Press*, vol. 9, pp. 23–27, 1997.
- [5] H. Lu, "Plane curve of constant width research," 2001.
- [6] T. Bayen and J.-B. Hiriart-Urruty, "Convex objects of constant width (in 2D) or thickness," *Annales des sciences mathématiques du Québec*, pp. 17–42, 2017.

- [7] H. L. Resnikoff, "On Curves and Surfaces of Constant Width," Apr. 2015, [Online]. Available: <http://arxiv.org/abs/1504.06733>
- [8] A. David Irving, "Curves of Constant Width & Centre Symmetry Sets," 2006.
- [9] C. Panraksa and L. C. Washington, "Real algebraic curves of constant width," *Period Math Hung*, vol. 74, no. 2, pp. 235–244, Jun. 2017, doi: 10.1007/s10998-016-0149-9.
- [10] L. Paciotti, "Curves of Constant Width and Their Shadows," 2010.
- [11] S. G. Dhande and Rajaram N., "Kinematic Analysis of Constant-Breadth Cam-Follower Mechanisms," *Journal of Mechanisms Transmissions and Automation in Design*, no. 106, pp. 214–221, 1984, [Online]. Available: <https://mechanicaldesign.asmedigitalcollection.asme.org>
- [12] Jinjiang Z., "Research on flat surface and constant width curve," 2001.
- [13] G. Figliolini and P. Rea, "Reuleaux Triangle and its Derived Mechanisms."
- [14] Yüzbaşı Ş. and Karaçayır M., "A Galerkin-like scheme to determine curves of constant breadth in Euclidean 3-space," *TWMS Journal of Applied and Engineering Mathematics*, vol. 11, no. 3, pp. 646–658, 2021, [Online]. Available: <https://orcid.org/0000-0001-6230-3638>.
- [15] H. Satoshi and T. Shun, "Development of a reduction mechanism integrated with a constant-breadth cam," in *Proceedings of JSPE Semestrial Meeting*, 2017.
- [16] L. Wang, W. Zhang, C. Wang, F. Meng, W. Du, and T. Wang, "Conceptual Design and Computational Modeling Analysis of a Single-Leg System of a Quadraped Bionic Horse Robot Driven by a Cam-Linkage Mechanism," *Appl Bionics Biomech*, 2019, doi: 10.1155/2019/2161038.
- [17] M. Asgari, E. A. Phillips, B. M. Dalton, J. L. Rudl, and D. L. Crouch, "Design and Preliminary Evaluation of a Wearable Passive Cam-Based Shoulder Exoskeleton," *JOURNAL OF BIOMECHANICAL ENGINEERING-TRANSACTIONS OF THE ASME*, vol. 144, no. 11, 2022, doi: 10.1115/1.4054639.
- [18] E. E. Zayas-Figueras and I. Buj-Corral, "Comparative Study about Dimensional Accuracy and Surface Finish of Constant-Breadth Cams Manufactured by FFF and CNC Milling," *Micromachines (Basel)*, vol. 14, no. 2, Feb. 2023, doi: 10.3390/mi14020377.
- [19] Artobolevsky I. I., *Mechanisms in Modern Engineering Design, A Handbook for Engineers, Designers and Inventors, Volume IV: Cam and Friction Mechanisms Flexible-Link Mechanisms*. Moscow: Mir Publishers, 1977.
- [20] V. I. Smirnov, "CHAPTER I ORDINARY DIFFERENTIAL EQUATIONS," in *A COURSE OF Higher Mathematics*, vol. 2, PERGAMON PRESS, 1964, pp. 32–36.
- [21] K. J. Waldron, G. L. Kinzel, and A. S. K., *Kinematics, Dynamics, and Design of Machinery*. Chichester: John Wiley & Sons Ltd, 2016.
- [22] E. Söylemez, *Mechanisms*. METU Publications, 1986.